The ERIS gvAPP Coronagraph: theoretical and on-sky performance

M. A. Kenworthy[1], F. Dannert[2], J. Hayoz TBD[2], D. Doelman[1], Ben Sutlieff[3], F. Snik[1], and S. Quanz[2]

[1] Leiden Observatory, University of Leiden, PO Box 9513, 2300 RA Leiden, The Netherlands
e-mail: kenworthy@strw.leidenuniv.nl

[2] ETH Zurich, Switzerland
[3] Edinburgh

Received August 21, 2024; accepted XXXX

ABSTRACT

Aims. We describe the gvAPP coroangraph for ERIS.
Methods. On sky observations from the commissioning run enabled characterisation of the gvAPP performance.
Results. Excellent matching with the prescribed pattern. Different wavelength performance.

Key words. instrumentation – coronagraphs

1. Introduction

The Enhanced Resolution Imager and Spectrograph for the VLT (ERIS; Davies et al. 2023) is an diffraction limited 1.5 to 5 micron imager and spectrograph, providing a 20 arcsecond field of view and $R = 5000$ spectroscopy using an integral field unit. It is composed of two parts, the integral field spectrograph SPIFFIER (REF) and the diffraction-limited high angular resolution imager NIX (REF).

2. Phase pattern design

MAK, DD

- The ERIS gvAPP designed in 2018
- The design steps follow Doelman et al. (2021)
- The design takes advantage of the small spiders and relatively small central obscuration with an aggressive design contrast at a small IWA.
- The vAPP is also a cold stop. To account for pupil wander and drifts, the pupil was undersized.
- The dark zones are broadened in the grating direction to account for wavelength smearing.
- The direction of the grating and dark zones was chosen to minimize the impact of spider diffraction in the dark zone, which would reduce the design Strehl ratio.
- The grating has 25 cycles over the diameter, resulting in a 25 λ/D separation between the coronagraphic PSF and the leakage term. This separation was chosen to minimize the impact of the leakage PSF intensity and account for the width of the dark zones.
- Lower-intensity reference PSFs the same separation but rotated 90 degrees have been added as an astrometric and photometric reference.
- The coronagraphic PSFs have additional dark zones underneath the leakage term and reference PSFs to reduce the impact of residual aberrations on their photometry.

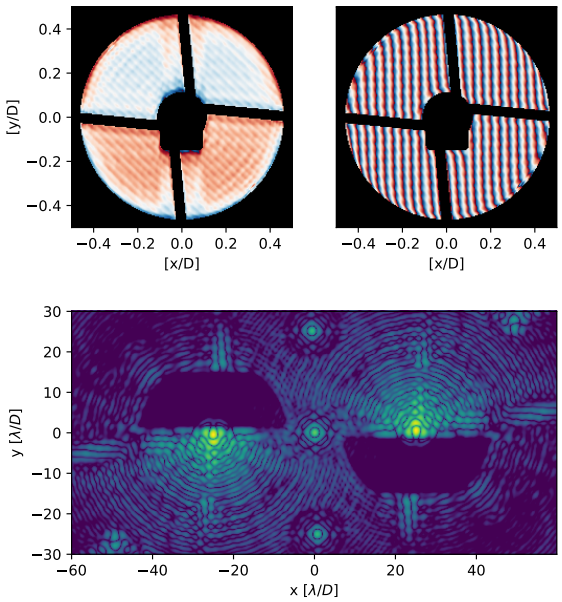

Fig. 1: The ERIS gvAPP phase pattern design and and simulated PSF.

Table 1: Design parameter values of the ERIS gvAPP

Design parameter	IWA	IWA contrast	OWA	OWA contrast	Strehl
	$[\lambda/D]$		$[\lambda/D]$		[%]
Value	2.2	10^{-4}	15	10^{-5}	50.9

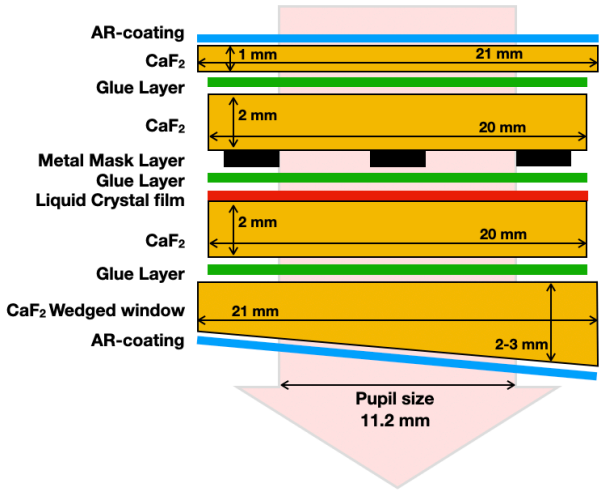

Fig. 2: The ERIS gvAPP optical layering.

3. Optical construction of the gvAPP

MAK, DD

- Component manufactured by ImagineOptix in 2018
- Two components manufactured, spare has slightly worse quality.

Optical layering, flatness, wedge

- The optics stack of the gvAPP consists of four individual substrates glued together.
- The number of substrates needed to be four due to manufacturing limitations and instrument constraints.
  - The AR-coating could not be applied to the opposite side of the aluminium mask.
  - The liquid-crystal film could not be applied on the wedged substrate.
- Amplitude mask is Aluminum thickness about 300 nm, OD > 4.
- The wedge is pointing North South, orthogonal to the grating
- The stack thickness is 7.55/7.39 mm (top, bottom), as measured with calipers. Resulting wedge angle is 0.44 degrees.
- The overall diameter is 20.95 mm.
- Centricity of clear aperture: Part A: 0.020 mm from center of 21 mm substrates
- Anti-reflection coatings are each $<$ 0.5 % average reflectance, verified by vendor
- Glue is NOA-61, aged 10-hrs at 50řC.

Transmission curve

- Both the glue and liquid crystal layers display absorption features in the thermal infrared and result in an average 2-5 μm transmission of 61.3%.
- The transmission was measured in the clear aperture and includes all substrates, glue layers, LCP layer, and anti-reflection coatings.
- A comparable transmission curve of the LBT dgvAPP can be found in Doelman et al. (2022).
- The overall transmission in is $\sim$ 90% in K-band, $\sim$ 50% in L-band, $\sim$ 40% in M-band.
- The absorption feature at 3.3μm goes to 0% transmission, rendering L-short observations ineffective. This absorption feature is caused by absorption in both the glue and liquid-crystal layers.
- The significant absorption in L-band and M-band will impact the gvAPP performance by increasing the photon noise of the thermal background.

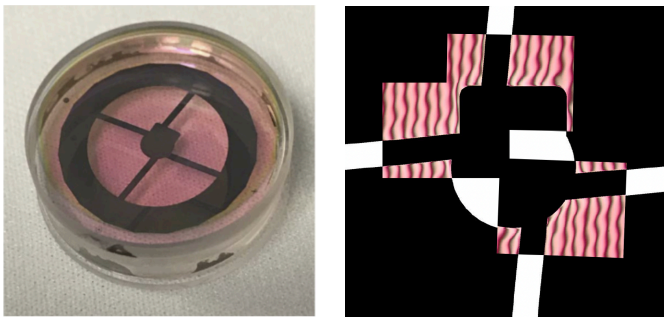

Fig. 3: Left: Image of the manufactured ERIS gvAPP. Right: Three stitched microscope images of the ERIS gvAPP between crossed polarizers. Images from ImagineOptix.

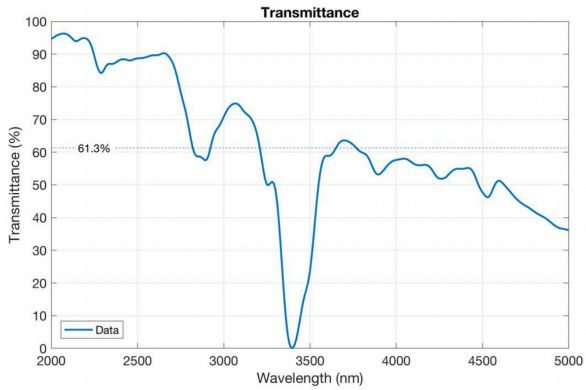

Fig. 4: Transmission of the gvAPP as a function of wavelength.

4. Summary cryogenic tests

MAK, DD

- gvAPP was tested at ETH Zurich cryogenic testbed (Boehle et al. 2018, 2021).
- The testbed was operated using a narrowband filter centered at 2.006 μm with a full width at half maximum of 0.045 μm.
- The first cryogenic tests confirmed that the morphology, overall throughput, and core intensity of the gvAPP PSF compared with a nominal VLT PSF is consistent with the theoretical predictions.
- After upgrades of the cryogenic testbed, it was discovered that the measured gvAPP PSF had a reduced dark zone contrast compared to the theoretical PSF. In the paper the authors find that the dark zone contrast was limited by the testbed itself instead of the gvAPP optical quality. The reduction in contrast can be explained by optical surface polishing errors with a power-law power spectral density, combine with some defocus and jitter.

Anne Boehle discussion from her paper

XXX TAKEN from ANNA's PAPER! This is David's original image...

Look at this photograph... Figure 5.

Glue throughput curve

Total throughput curve

5. On-sky PSF comparison with model PSF

5.1. narrow band PSF on-sky

5.2. Current measured on-sky

JH, FD

5.3. IB on sky

JH, FD

DD to meet with Ben Sutlieff Friday 14:00

left/right PSF brightness is not the same. hints at circular instrumentation systematics in ERIS???

Structure in the telescope pupil shows striping similar to the grating for the gvAPP - DD confirmed in 15/08/2024 email that these fringes are in the pattern (they create the reference holograms), and so a bit of Fresnel propagation will likely give the intensity variations.

Should look into why the spiders are so much thicker and what the bright ring is. Suspect this not only Fresnel propagation.

5.4. Wavelength performance predicted and measured

JH, FD, MAK

6. Contrast curves

6.1. Current measured on-sky

JH, FD, DD, BS

Include K-peak data from B.S.

6.2. Predicted performance for broad bands

JH, FD, DD Idea: take the contrast curve in K-peak (from BS), extrapolate it to the Kband (using the higher bandpass, and ignoring the changing sky background).

7. Conclusions

- gvAPP works to the design described, beamswitches perfectly, very easy to use.
- gvAPP successfully pushes diffraction halo below the wind driven halo from the atmosphere and AO system performance.
- L band limited by large sky background from warm optics in ERIS optical path and poor transmission due to multiple glue layers in ERIS gvAPP.
- Detector pattern noise and artifacts limit the K band reduction
- Future ELT instruments will minimise glue layers and increase strehl ratio for the same PSF contrast to improve planet throughput.

7.1. Impact on future designs for ELT class telescopes

Ask Olivier and Gilles

Everyone!

Minimise the number of glue layers (2 is probably minimum)

Acknowledgements. ADD YOUR ACKNOWLEDGEMENTS HERE This research has used the SIMBAD database, operated at CDS, Strasbourg, France (Wenger et al. 2000). This work has used data from the European Space Agency (ESA) mission *Gaia* (https://www.cosmos.esa.int/gaia), processed by the *Gaia* Data Processing and Analysis Consortium (DPAC, https://www.

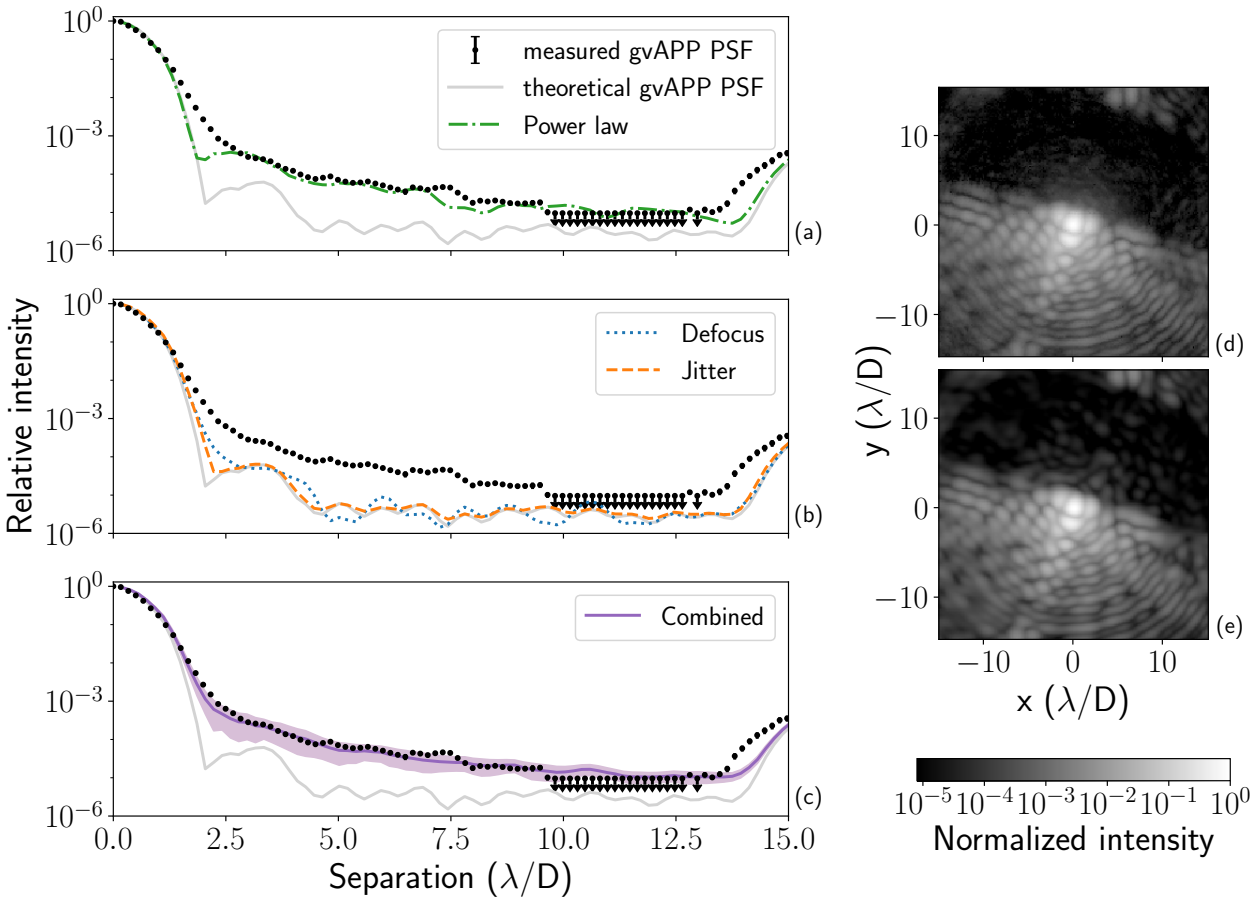

Fig. 5: Results from the simulations of the aberrations observed in the gvAPP PSF. The left column displays the simulated contrast curves when applying a a single realization of a power law aberration to simulate polishing errors (panel a), defocus and jitter aberrations (panel b), and all 3 aberrations combined including the average of 100 power law realizations and the 1σ spread (panel c). Each simulated contrast curve is compared to the data (black points) and to the theoretical gvAPP PSF (gray line). The right column shows the test bench data of the left gvAPP PSF (panel d) compared to the simulated PSF with all 3 aberrations included (panel e). We find that including polishing errors adds flux to the gvAPP dark hole as seen in the test bench measurements and that adding defocus and jitter smooths the PSF and makes the inner and outer edges of the dark hole line up with the measurements. The combination of all three aberrations can explain the data very well in terms of the contrast curve and the PSF morphology.

cosmos.esa.int/web/gaia/dpac/consortium). Funding for the DPAC has been provided by national institutions, in particular the institutions participating in the *Gaia* Multilateral Agreement. To achieve the scientific results presented in this article we made use of the *Python* programming language[1], especially the *SciPy* (Virtanen et al. 2020), *NumPy* (Oliphant 2006), *Matplotlib* (Hunter 2007), *emcee* (Foreman-Mackey et al. 2013), and *astropy* (Astropy Collaboration et al. 2013, 2018) packages.

References

Astropy Collaboration, Price-Whelan, A. M., Sipőcz, B. M., et al. 2018, AJ, 156, 123
Astropy Collaboration, Robitaille, T. P., Tollerud, E. J., et al. 2013, A&A, 558, A33
Boehle, A., Doelman, D., Konrad, B. S., et al. 2021, Journal of Astronomical Telescopes, Instruments, and Systems, 7, 045001
Boehle, A., Glauser, A. M., Kenworthy, M. A., et al. 2018, in Society of Photo-Optical Instrumentation Engineers (SPIE) Conference Series, Vol. 10702, Ground-based and Airborne Instrumentation for Astronomy VII, ed. C. J. Evans, L. Simard, & H. Takami, 107023Y
Davies, R., Absil, O., Agapito, G., et al. 2023, A&A, 674, A207
Doelman, D. S., Snik, F., Por, E. H., et al. 2021, Appl. Opt., 60, D52
Doelman, D. S., Stone, J. M., Briesemeister, Z. W., et al. 2022, AJ, 163, 217
Foreman-Mackey, D., Hogg, D. W., Lang, D., & Goodman, J. 2013, PASP, 125, 306
Hunter, J. D. 2007, Computing in Science and Engineering, 9, 90
Oliphant, T. E. 2006, A guide to NumPy, Vol. 1 (Trelgol Publishing USA)
Virtanen, P., Gommers, R., Oliphant, T. E., et al. 2020, Nature Methods, 17, 261
Wenger, M., Ochsenbein, F., Egret, D., et al. 2000, A&AS, 143, 9

[1] Python Software Foundation, https://www.python.org/

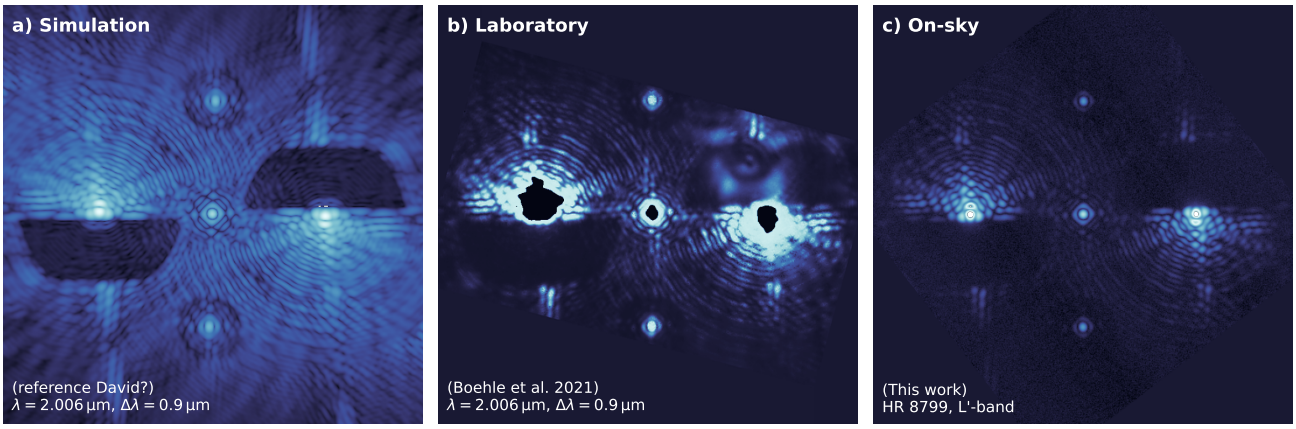

Fig. 6: Todo.

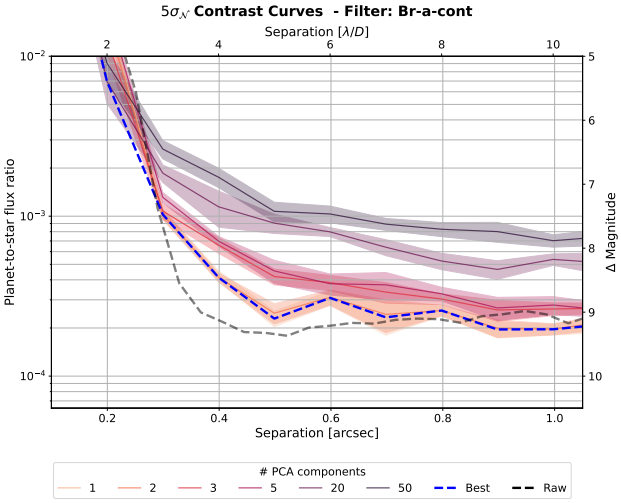

Fig. 7: Todo.